



Corrosion Inhibition of Sodium Silicate with Nanosilica as Coating in Pre-Corroded Steel

Marish S. Madlangbayan ^{1*}, Carlo Nico B. Diola ¹, Alvin Karlo G. Tapia ²,
Milagros M. Peralta ³, Engelbert K. Peralta ⁴, Ronaniel A. Almeda ⁴,
Maris Asuncion L. Bayhon ⁴, Marloe B. Sundo ¹

¹ Department of Civil Engineering, University of the Philippines Los Baños, Laguna 4031, Philippines.

² Institute of Mathematical Sciences and Physics, University of the Philippines Los Baños, Laguna 4031, Philippines.

³ Institute of Chemistry, University of the Philippines Los Baños, Laguna 4031, Philippines.

⁴ Institute of Agricultural and Biosystems Engineering, University of the Philippines Los Baños, Laguna 4031, Philippines.

Received 02 August 2021; Revised 09 October 2021; Accepted 21 October 2021; Published 01 November 2021

Abstract

This study was conducted to investigate the potential of using sodium silicate with nanosilica as a treatment to inhibit the progress of corrosion in steel specimens that are already corroded. Steel specimens measuring 16 mm in diameter and 4 mm in thickness were prepared and subjected to pre-corrosion by immersion to 3.5% NaCl solution. Two sets of specimens were then dip-coated with sodium silicate containing nanosilica. One set was coated with 1% nanosilica, and the other was coated with 2.5% nanosilica. The coated specimens were then subjected to Complex Impedance Spectroscopy (CIS) at 20 Hz to 20 MHz frequency range. Compared with the sodium silicate coating with 1% nanosilica, the sodium silicate coating with 2.5% nanosilica had a larger semi-circle curve in the Nyquist plot. Similarly, the sodium silicate coating with 2.5% nanosilica also showed larger magnitudes of impedance at the low-frequency region and larger phase angles at the high-frequency regions in the Bode plot. These results imply that the sodium silicate coating with 2.5% nanosilica coating demonstrated better capacitive behavior. In addition, equivalent circuit modelling results also showed that the sodium silicate coating with 2.5% nanosilica had higher coating resistance and lower coating capacitance as compared to the sodium silicate coating with 1% nanosilica.

Keywords: Corrosion; Coating; Nanosilica; Impedance Spectroscopy.

1. Introduction

Corrosion is an electrochemical action that is primarily due to chloride ingress. Corrosion of structural elements affects different structures in various ways. In reinforced concrete structures, corrosion products or rust accumulate as corrosion-causing contaminants enter the concrete and reach the reinforcing steel bars. These accumulated corrosion products cause internal stress which leads to concrete cracking or spalling. Corrosion in steel structures causes reduction in the area of the structural members, leading to lower resistance to stresses [1]. On a global scale, damages that are caused by corrosion are approximately \$276 billion per year [2]. An example of which was the repair and

* Corresponding author: msmadlangbayan@up.edu.ph

 <http://dx.doi.org/10.28991/cej-2021-03091761>



© 2021 by the authors. Licensee C.E.J, Tehran, Iran. This article is an open access article distributed under the terms and conditions of the Creative Commons Attribution (CC-BY) license (<http://creativecommons.org/licenses/by/4.0/>).

demolition of Silver bridge in Ohio, USA, in 1967 [3]. With a 17.8% increase in the price index of steel from 2012 to 2018 [4], protection of existing structures against corrosion damages has been the more viable option over reconstruction.

The most commonly used method in treating corroded steel is through the use of blasting and application of epoxy coating. Blasting uses abrasive materials to remove the existing rust produced by corrosion, therefore effectively cleaning the steel substrate [5]. It is also effective in removing contaminants on the steel surface, such as oil and grease. Furthermore, blasting creates a profile on the steel surface that is suitable for applying the protective coating. After blasting, application of the protective coating follows. Coatings such as epoxy coating act like a barrier preventing the intrusion of harmful elements like chlorides that causes corrosion of the steel. It also provides a resistant media between the anodic and cathodic portions found on the steel surface [6-7]. This protective property of coating is important because defects on a coated steel surface are difficult to prevent. Once a defect is formed on the coated surface, corrosion process can occur between the defect area and the sound portions. The progress of this type of corrosion process will be dependent on the resistance of the coating used [8-9].

Inorganic material-based nanoparticles have been extensively studied as effective and more environmentally friendly coating components for the past years. Past research works explored the use of various nanoparticles, such as Fe_2O_3 , ZrO_2 , ZnO , and SiO_2 , to enhance the mechanical properties of anti-corrosion composite coatings [10-13]. In a study by Khan et al. [14] for epoxy-based coatings, it was found out that among the nanoparticles, nanosilica increased the hardness and elastic modulus the most by 71% and 26%, respectively.

Nanosilica has been used to enhance the properties of composites due to its structure and morphology [15]. Rice Hull Ash (RHA), an agro-industrial waste from rice production, contains over 90% nanosilica thereby making extraction of nanosilica from RHA highly cost-efficient [16-17]. Studies also have shown that nanosilica can prevent corrosion through the formation of a silicate network [18]. Its nanoscale size allows it to penetrate small voids formed by corrosion products. Moreover, high surface area causes nanosilica to be easily dissolved in a media that contributes to silicate network formation's uniformity [19]. The silicate network forms thin layers that can act as a physical barrier that prevents chlorides and contaminants that may initiate corrosion. Alkali silicate anti-corrosion coating is also known as silicate conversion coating. It is one example of an alkali-treated anti-corrosion coating. The structure of the coating contains polymeric particles such as silanol groups (Si-OH) and siloxane bridge (Si-O-Si) [20]. During the curing process, the polymerization continued and more siloxane groups were converted to siloxane bridges [21].

Dela Cruz et al. [22] studied the use of nanosilica and polyaniline (PANI) composites in epoxy coated steel specimens. The study showed that all percent combinations of nanosilica and PANI composites in the epoxy coating have better corrosion protection performance compared to that of pure epoxy coated steel by yielding higher coating resistance and lower coating capacitance. Among the different percent combinations of nanosilica-PANI, the 40-60% combination of nanosilica and PANI exhibited the highest coating resistance and lowest coating capacitance. In another study, the group of Ruzgal [23] investigated the effect of nanosilica when used as a coating enhancer for cold-rolled steel. Their study demonstrated that nanosilica-enhanced coating reduced soil-to-metal friction and soil adhesion for cold-rolled steel by 24% and 36%, respectively.

To evaluate the performance of coatings and corrosion activity in steel, researchers use a non-destructive technique called Complex Impedance Spectroscopy (CIS). Through CIS technique, the impedance at different frequencies can be measured. The impedance data, particularly those found at the low-frequency region, can characterize the coating resistance and capacitance. At the same time, the impedance data can be used to determine the rate of corrosion of the substrate steel underneath the coating and the failure mechanism of coating systems. The CIS technique was used in this study.

Research on the use of sodium silicate with nanosilica, synthesized from RHA, as a treatment for corroded steel is scarce. This study aims to contribute knowledge and understanding on the potential capability of sodium silicate, with nanosilica from RHA, in treating corroded steel by inhibiting further progress of corrosion. The specific objectives of the study are: (1) to characterize the effectiveness of sodium silicate coating with nanosilica applied to pre-corroded steel by examining the generated Nyquist and Bode plots and (2) to determine the resistance and capacitance of sodium silicate coating with nanosilica using Equivalent Circuit Modelling.

This paper is structured as follows: materials and methods are discussed in section 2. It is in this section where the material properties, preparation of specimens and test methods are presented in detail. In section 3, the results of Nyquist and Bode plots are presented and discussed together with the results of the equivalent circuit modelling. Section 4 presented the conclusions of the study.

2. Materials and Methods

In this study, the corrosion inhibition of sodium silicate with nanosilica synthesized from RHA was evaluated by using CIS in coated steel specimens. The steps for evaluation are shown in Figure 1.

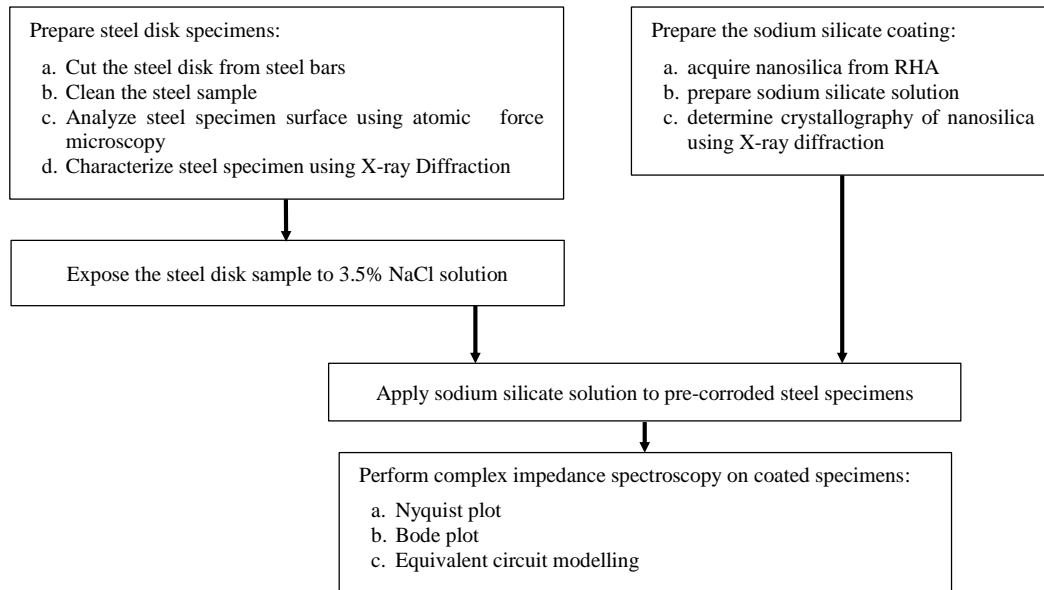


Figure 1. Flowchart of the research methodology

2.1. Materials Used

2.1.1. Steel

Round steel bars that are locally and commercially available were used in the study. Initially, round bars of 16 mm diameter were cut into 4mm thick coupons and were subjected to surface preparation in accordance with ASTM G1 standard method [24]. Briefly, existing rusts, dirt, and oil were removed by mechanical abrasion with using no. 100 sand paper and subsequently washing with distilled water and acetone. Representative sample specimens used in this study are shown in Figure 2.



Figure 2. Sample steel specimen used

Morphological and topographic nanoscale analysis were done using the XE-70 atomic force microscope in non-contact mode on the steel specimen's surface. Non-contact cantilever with resonant frequency of 330 kHz, force constant of 42 N/m, length of 125 μm , mean width of 30 μm and thickness of 4 μm were used in the analysis. Various scanning areas of 45 \times 45 μm in size at different portions of the steel specimen surface were obtained at a scan rate of 0.30 Hz.

The analysis of the steel specimen (Figure 3) showed uniform striations and a smooth surface. It was also observed that there are grooves present on its surface, possibly caused by surface preparation through mechanical abrasion using SiC abrasive paper. Presence of bulbous material was immediately observed possibly indicating that a rapid corrosion formation on the carbon steel surface was taking place. This phenomenon is frequently observed on an air-exposed steel surface.

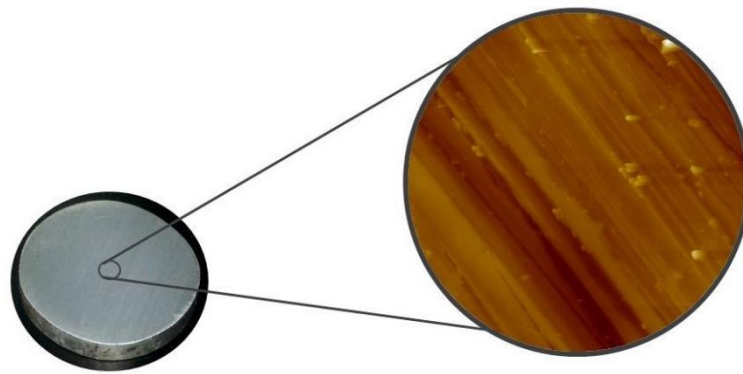


Figure 3. AFM analysis of clean steel specimen

X-ray diffraction analysis was done to further characterize the steel specimen. Shimadzu XRD-6100 equipped with an x-ray source with a copper target (wavelength 1.540598 Å) and has an accelerating voltage of 30 kV with a scan rate of 2° per minute and a scan range of 2° to 90° was used. Post-run analyses were done using X'Pert HighScore Plus software. Figure 4 shows the X-ray diffractogram of a clean steel sample.

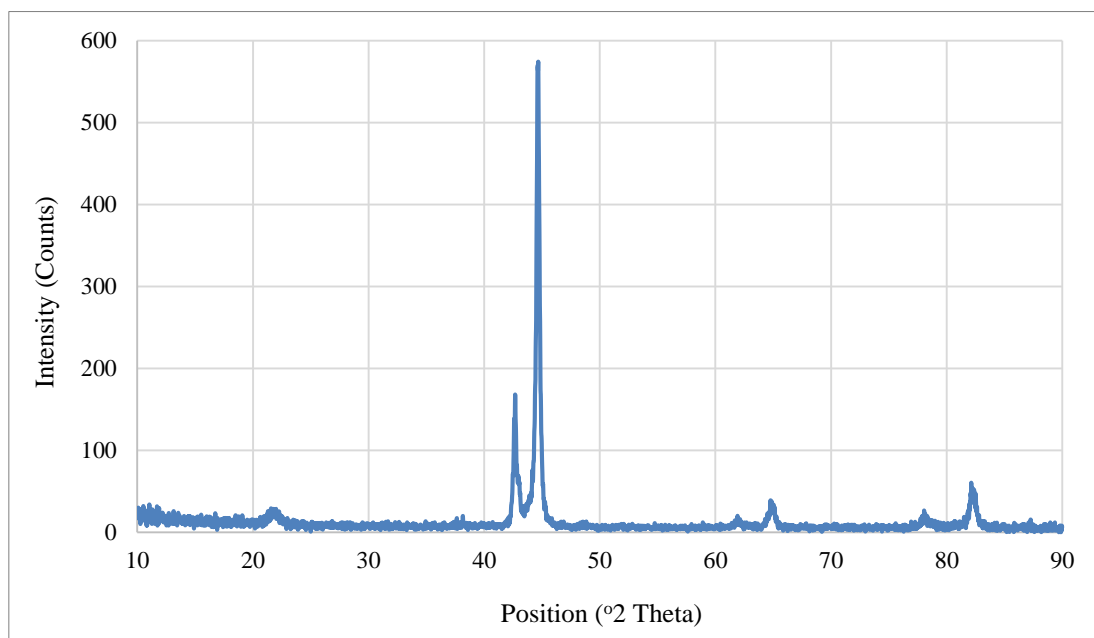


Figure 4. X-ray diffractogram of clean metal disc sample

2.1.2. Nanosilica

The nanosilica, shown in Figure 5, was synthesized from RHA using the technology developed by the group of Dr. Engelbert Peralta from the College of Engineering and Agro-Industrial Technology of the University of the Philippines Los Baños. The physical properties of nanosilica are summarized in Table 1.

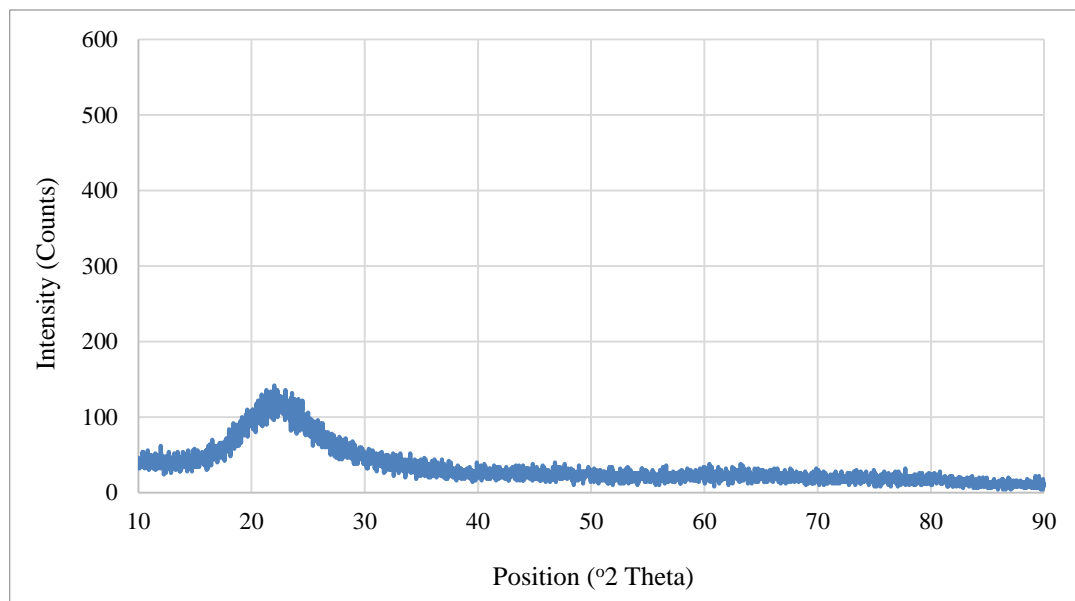


Figure 5. Powdered amorphous nanosilica synthesized from RHA

Table 1. Physical properties of the nanosilica used in the study

Property	Value
Average Particle Size	24.39 ± 0.38 nm
Surface Area	$\sim 260 - 300$ m ² /g
Pore Radius	$\sim 16 - 19$ Angstrom
Pore Volume	~ 0.246 cc/g

The crystallography of the nanosilica was determined through X-ray Powder Diffraction (XRD). In contrast to the crystallographic analysis of crystalline silica, which peaked at 22° , the crystallographic analysis of the powdered nanosilica used in this study (Figure 6) showed no peak at 22° . This means that the powdered nanosilica used in this study is highly amorphous. In addition, the presence of other contaminants was not observed, which means that the powdered nanosilica used in this study was also highly pure.

**Figure 6. Crystallographic analysis of the powdered nanosilica used in the study**

2.2. Pre-corrosion of Test Specimens

The cleaned steel samples were pre-corroded by exposing them to 3.5 (weight to volume) % NaCl solution. The samples were submerged in the solution for three days and then air-dried for one day. The pre-corroded steel sample specimen is shown in Figure 7.

**Figure 7. Pre-corroded steel specimen**

2.3. Preparation Of Sodium Silicate Solution

The nanosilica was oven-dried for 24 hours at 150°C to remove existing moisture. It was then cooled to room temperature. Desiccators were used to ensure a dry environment for the nanosilica. While cooling the nanosilica, a 3M

NaOH solution was formulated. Two 100mL NaOH solutions were used to dissolve 1.0 and 2.5 grams of nanosilica. The solutions were heated for 20 minutes at 80°C. The solutions were then cooled to room temperature.

2.4. Application of Coating in Test Specimen

The specimens were coated with sodium silicate containing nanosilica using dip-coating method with a submersion time of 30 minutes. The coated specimens were then oven-dried at 100°C for 20 minutes.

2.5. Impedance Measurement using CIS

Using an Impedance Analyzer shown in Figure 8, the test specimen’s real and imaginary impedance components were measured and recorded at varying frequencies (20 to 20 MHz). The impedance spectra evolution through time was derived from the assessment of the coating’s impedance using CIS. The total impedance was measured and noted which follows Ohm’s law defined by Equation 1.

$$Z(\omega) = \frac{V(\omega)}{I(\omega)} = Z_{real}(\omega) + Z_{img}(\omega)j \tag{1}$$

CIS was used to generate the Nyquist and Bode plot of the respective coatings. The Nyquist plot was formed by plotting the imaginary impedance component in the y-direction and the real impedance component on the x-direction. On the other hand, the Bode plot was obtained by plotting in a logarithmic scale the total impedance measured at varying frequencies from 20 Hz to 20 MHz. The total impedance was computed using Equation 2.

$$|Z(\omega)| = \sqrt{Z_{real}(\omega)^2 + Z_{img}(\omega)^2} \tag{2}$$

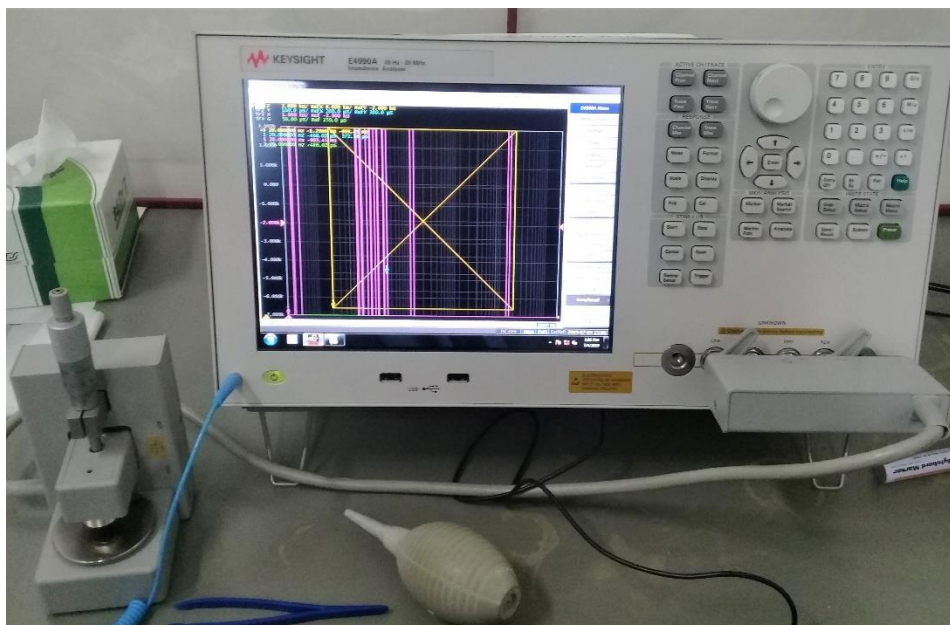


Figure 8. Impedance Analyzer used in the study

ECM was used to quantify the coating resistance and coating capacitance using EC Lab as the fitting software and Igor as the plotting software. From the total impedance components measured using CIS, the Nyquist plot was generated. Using the Z-fit feature of EC Lab 10.40, the ECM’s graph was fitted to the actual Nyquist plot. The equivalent circuit used to determine the values of each electrical component, particularly the coating resistance and capacitance, is shown in Figure 9.

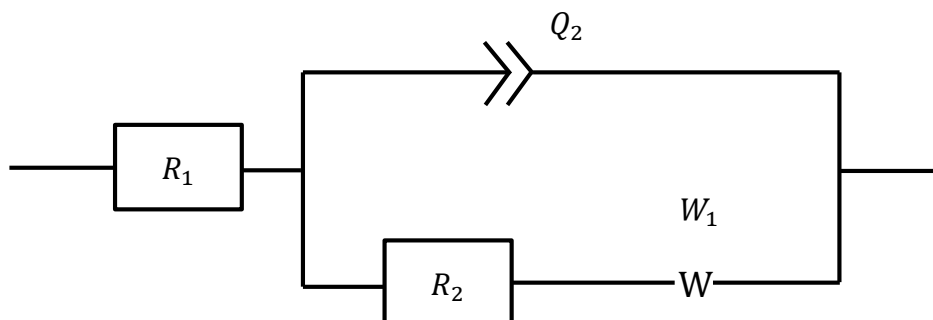


Figure 9. Equivalent circuit used in the study

3. Results and Discussion

3.1. Nyquist Plot

CIS was employed to evaluate the corrosion inhibition of the sodium silicate coating with 1% and 2.5% concentration of nanosilica. The real and imaginary values of the impedances were plotted to obtain the Nyquist plots. Using the Nyquist plot, the coating performance can be interpreted through the position and size of the diameter of the semi-circle formed. The semi-circle plot showing an almost vertical behavior near the vertical axis, and that with a larger diameter signifies better coating performance.

Figure 10 shows the Nyquist plots of sodium silicate coated steel obtained with 1 and 2.5% nanosilica. The Nyquist plot for the sodium silicate coated steel containing 2.5% nanosilica show more vertical behavior and larger diameter thus demonstrating better quality compared to the coating with 1.0% nanosilica. It illustrates the capacitive behavior of the coating commonly observed in coated steel substrate that is not experiencing corrosion. On the other hand, the Nyquist plot for the sodium silicate coated steel containing 1.0% nanosilica shows a more depressed loop. A Warburg impedance started to appear as a diagonal line at the end of the loop which demonstrates diffusion induced behavior. With this observation, it is important to include a Warburg element in the equivalent circuit model during curve fitting.

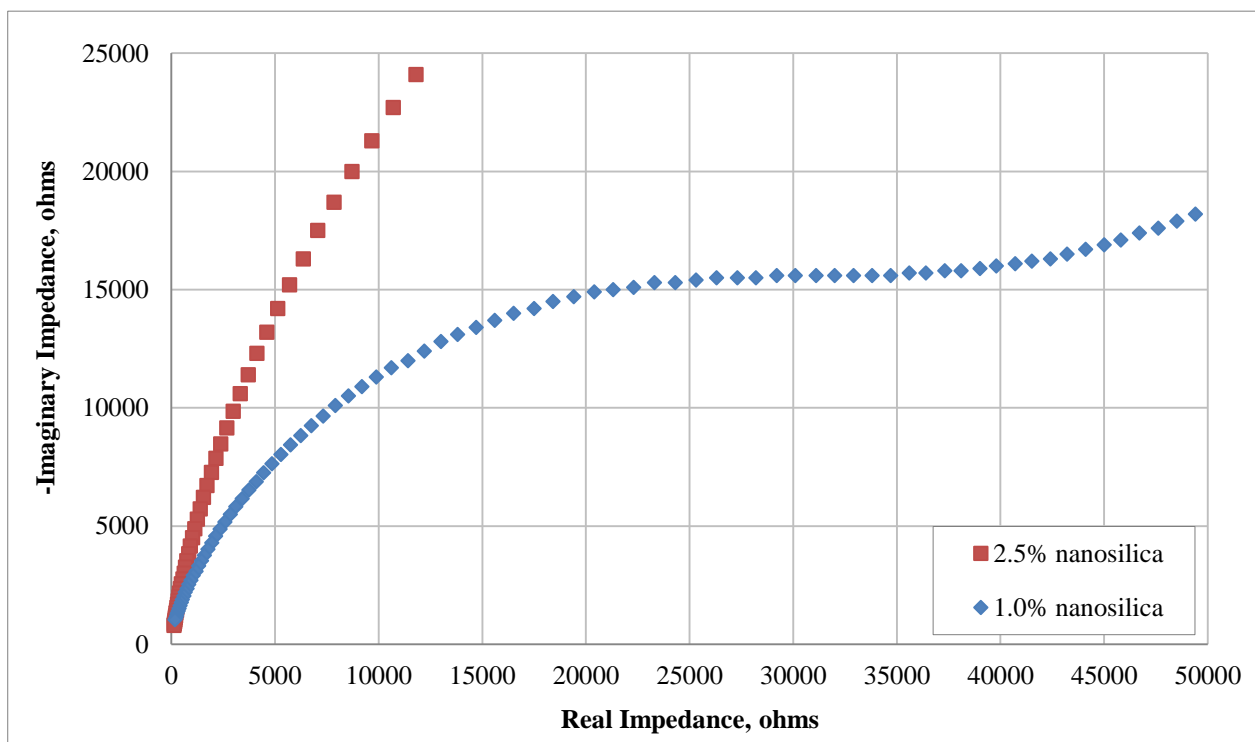


Figure 10. Nyquist plot of coated steel specimens

3.2. Bode Plot

The Bode plot was generated by plotting the logarithm of the impedance modulus and the phase angle displacement as functions of the logarithm of frequency. The impedance modulus and phase angle displacement at different frequencies are shown in Figures 11 and 12, respectively. It can be observed that the coating with 2.5% nanosilica exhibited higher impedance values at the low-frequency region and higher phase angle at the high-frequency region as compared to the coating with 1.0% nanosilica. Therefore, the coating with 2.5% nanosilica exhibited a more capacitive behavior compared to the coating with 1.0% nanosilica.

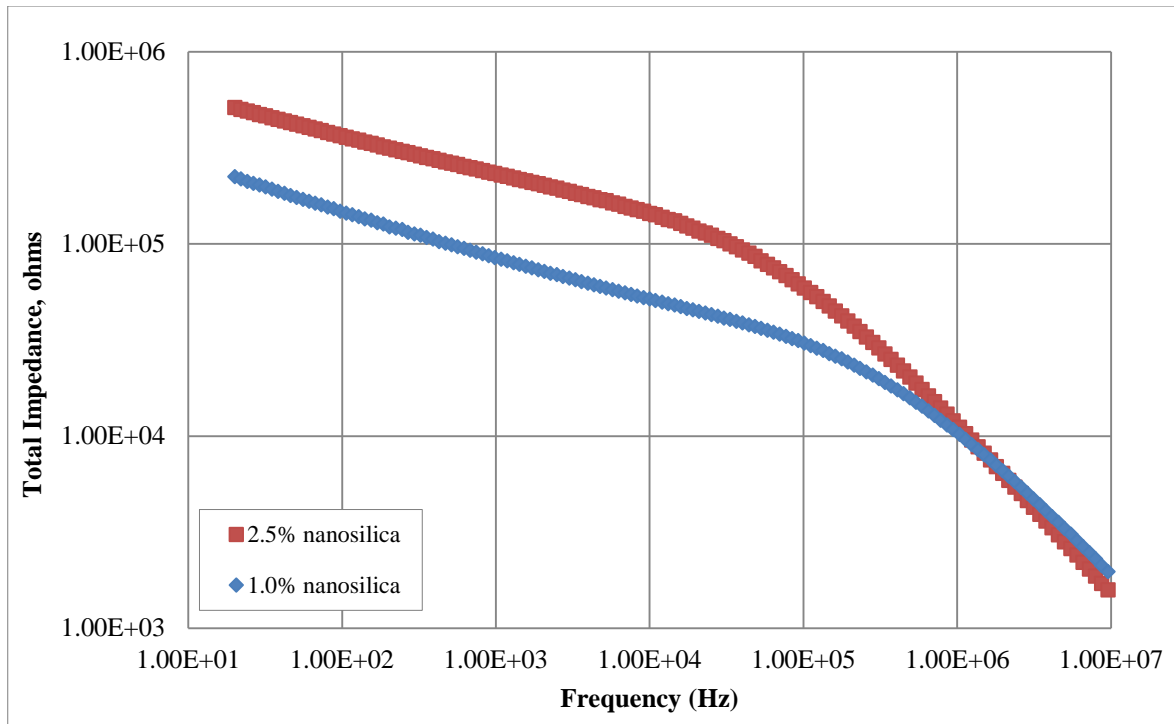


Figure 11. Bode plots of coated steel specimens

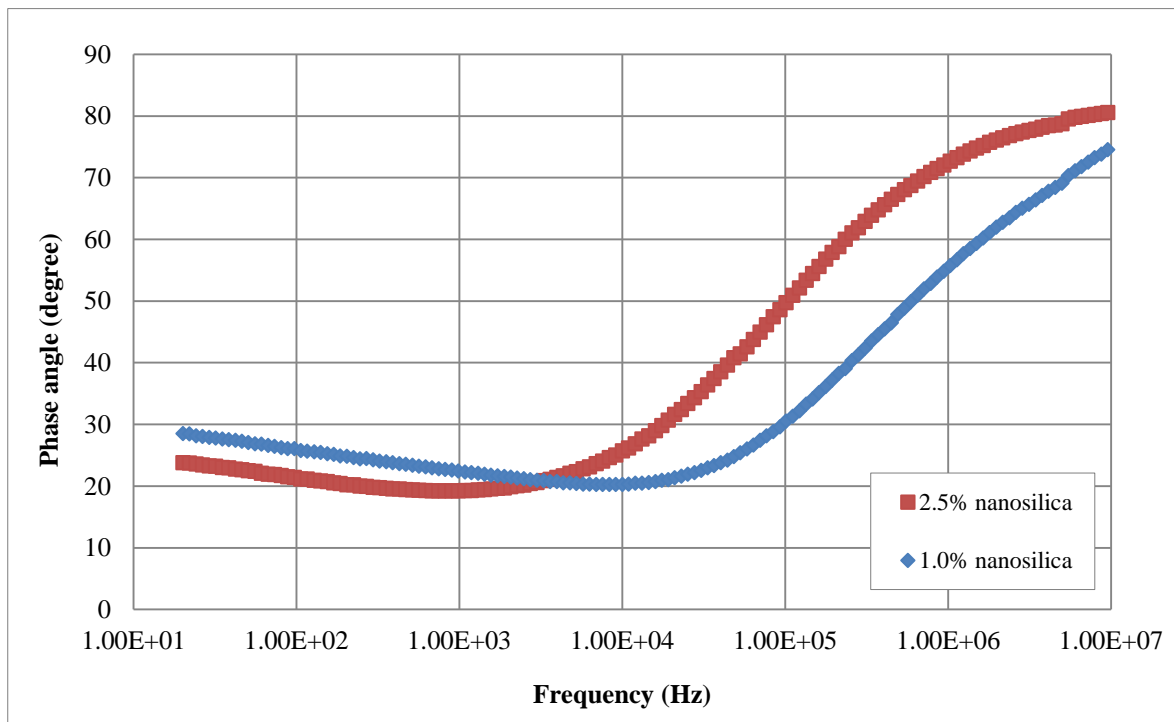


Figure 12. Phase angle data generated from CIS

3.3. Equivalent Circuit Model

Equivalent circuit model-fitting has been used as a powerful technique to get insights into the properties of a variety of materials [25]. The CIS data of the coating systems were fitted graph of the equivalent circuit in order to calculate the values of coating capacitance (C_c) and coating resistance (R_c). The curve fitting is shown in Figure 13 while the computed values of the coating capacitance and coating resistance are shown in Table 2. The sodium silicate coating containing 2.5% nanosilica showed lower capacitance than the 1% nanosilica coating. This indicates that the coating with 2.5% nanosilica has a lower electrolyte intake and is less porous than the 1% nanosilica coating. In addition, a higher coating resistance was observed for the sodium silicate coating containing 2.5% nanosilica. The increase in resistance was found to be one order in magnitude. This indicates that the coating with 2.5% nanosilica has a better corrosion inhibition for the steel substrate.

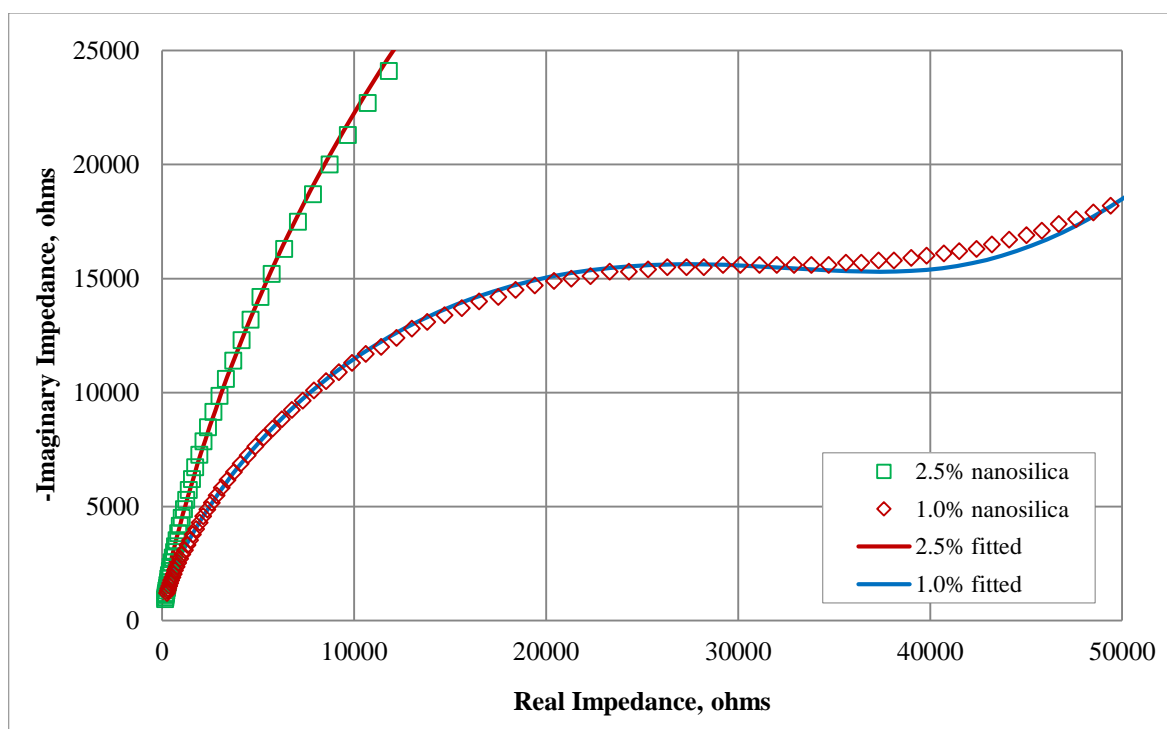


Figure 13. Curve fitting using the equivalent circuit model

Table 2. Coating capacitance and resistance values

	Cc (Farads)	Rc (Ohms)
1.0% NanoSiO ₂	2.37 E-09	4.38 E+04
2.5% NanoSiO ₂	2.93 E-10	1.16 E+05

In this study, the steel substrate was already subjected to corrosion prior to application of sodium silicate with nanosilica as coating. Therefore, it is important to note that the surface of the substrate is already non-uniform and contains crevices and voids as a consequence of the induced corrosion. Without a barrier protection, these crevices and voids will serve as venues where local corrosion can occur and progress.

The sodium silicate coating used in this study formed a thin layer of hardened paste on the surface of the corroded steel substrate. This finding is in congruence with the work of Ruzgal et al. [23] where the hardened paste composed of silica hydrates had a tendency to be accumulated and deposited in the crevices of the steel substrate. The tendency of the sodium silicate hydrate to fill the crevices present in the steel substrate is due to its high surface area-volume ratio. The accumulation of silica in the crevices provides an indicative explanation why the coating with 2.5% nanosilica exhibited better corrosion inhibition performance compared with the coating with only 1% nanosilica.

4. Conclusion

The study investigated the performance of sodium silicate on preventing the progress of corrosion in pre-corroded steel specimens. CIS technique was used to evaluate and compare the coating performance of sodium silicate with 1 and 2.5% nanosilica derived from RHA. Both the Nyquist plot and Bode plots provided evidence that the sodium silicate with 2.5% nanosilica derived from RHA has prevented the progress of corrosion in coated steel plates. The Nyquist plot for the sodium silicate with 2.5% nanosilica exhibited a semi-circle with a larger diameter than the semi-circle plotted using the coating with only 1% nanosilica. These results exemplify a capacitive coating behavior. In terms of the Bode plot, the sodium silicate with 2.5% nanosilica exhibited a higher magnitude of impedance at the low-frequency region and larger phase angles at the high-frequency regions, which are also indicators of a capacitive behavior. Equivalent circuit modelling enabled the comparison of the values of coating resistance and coating capacitance of sodium silicate with nanosilica derived from RHA. Sodium silicate with 2.5% nanosilica had a higher coating resistance by one order in magnitude. In terms of coating capacitance, the coating with 2.5% nanosilica also showed lower capacitance indicating that it has lower electrolyte intake and is less porous compared to the coating with only 1% nanosilica. The study therefore has provided evidence that sodium silicate with nanosilica derived from RHA can inhibit the further progress of corrosion in steel substrate. In addition, sodium silicate with 2.5% nanosilica derived from RHA performs better than a sodium silicate with only 1% nanosilica derived from RHA in inhibiting the progress of corrosion in steel substrate.

5. Declarations

5.1. Author Contributions

Conceptualization, M.S.M. and C.N.B.D.; methodology, M.S.M., C.N.B.D., A.K.G.T., M.M.P. and R.A.A.; formal analysis, M.S.M., A.K.G.T., M.M.P., E.K.P. and M.B.S.; investigation, C.N.B.D., R.A.A., M.A.L.B. and A.K.G.T.; writing—original draft preparation, M.S.M., C.N.B.D. and R.A.A.; writing—review and editing, M.S.M., C.N.B.D., R.A.A., M.B.S., M.A.L.B., M.M.P. and E.K.P. All authors have read and agreed to the published version of the manuscript.

5.2. Data Availability Statement

The data presented in this study are available in article.

5.3. Funding

This work is primarily funded by the Philippine Council for Industry, Energy and Emerging Technology Research and Development, Department of Science and Technology with Project No. 03713, 2020.

5.4. Conflicts of Interest

The authors declare no conflict of interest.

6. References

- [1] Melchers, Robert E. "The Effect of Corrosion on the Structural Reliability of Steel Offshore Structures." *Corrosion Science* 47, no. 10 (October 2005): 2391–2410. doi:10.1016/j.corsci.2005.04.004.
- [2] Gowda, S. "Multi-scale effects of corrosion on steel structures." Unpublished Doctorate Dissertation, University of Akron, Akron, USA. (December 2016).
- [3] Petrovic, Zoran. "Catastrophes Caused by Corrosion." *Vojnotehnicki Glasnik* 64, no. 4 (2016): 1048–1064. doi:10.5937/vojtehg64-10388.
- [4] Tapia, M. "The Rising Cost of Construction Materials." *BEXazbex*, (June 2019). Available online: <https://azbex.com/the-rising-cost-of-construction-materials/> (accessed on March 2021).
- [5] Corpro System. "Abrasive Blasting." (July 2019). Available online: <https://www.cor-pro.com/corrosion-protection-services/abrasive-blasting/> (accessed on March 2021).
- [6] Hayatdavoudi, H and Rahsepar, M., "A mechanistic study of the enhanced cathodic protection performance of graphene-reinforced zinc rich nanocomposite coating for corrosion protection of carbon steel substrate" *Journal of Alloys and Compounds* 727 (August 2017): 1148-1156. doi:10.1016/j.jallcom.2017.08.250.
- [7] Duong, N.T., Hang, T.T.X., Nicolay, A., Paint, Y. and Olivier M.G., "Corrosion protection of carbon steel by solvent free epoxy coating containing hydrotalcites intercalated with different organic corrosion inhibitors." *Progress in Organic Coatings* 101 (September 2016): 331-341. doi:10.1016/j.porgcoat.2016.08.021.
- [8] Madlangbayan, Marish S., Nobuaki Otsuki, Takahiro Nishida, and Tsuyoshi Saito. "Investigation on the Corrosion of Coated Steel Plates with Impact Defect Using Divided Steel Plates." *Civil Engineering Journal* 4, no. 1 (February 7, 2018): 58. doi:10.28991/cej-030968.
- [9] Otsuki, N., Min, A.K., Madlangbayan, M.S. and Nishida, T. "A Study on Corrosion of Paint-Coated Steel with Defects in Marine Environment." *Doboku Gakkai Ronbunshuu E* 63, (December 2007): 667-676. doi:10.2208/jsceje.63.667.
- [10] Abbasi; M., Attar, M. M. "Investigation of Anti-Corrosion and Adhesion Properties of Epoxy Coatings Containing Surface Modified Fe₂O₃ Nano Particles on Mild Steel." *Nace Corrosion 2019*, Nashville, Tennessee, USA, (March 2019).
- [11] Stambolova I, Boshkov NS, Boshkova N, Stoyanova D, Shipochka M, Simeonova S and Grozev N. "Environmentally Friendly Anticorrosive Layered Zirconia/Titania/Low-Carbon Steel Structures." *Materials Proceedings*. 2021, 4, 75. doi:10.3390/IOCN2020-07791.
- [12] Aboorvakani R, Vethanathan SJK and Madhuc KU. "Influence of Zn concentration on zinc oxide nanoparticles and their anti-corrosion property." *Journal of Alloys and Compounds* 834, (2020) 155078. doi:10.1016/j.jallcom.2020.155078
- [13] Liang T, Yuan H, Li C, Dong S, Zhang C, Cao G, Fan Y, Zhao X and Cao X. "Corrosion inhibition effect of nano-SiO₂ for galvanized steel superhydrophobic surface." *Surface and Coatings Technology* 406, (2021) 126673. doi:10.1016/j.surfcoat.2020.126673.
- [14] Khan, R., Azhar, M.R., Anis, A., Alam, M.A., Boumaza, M., and Al-Zahrani, S.M. "Facile synthesis of epoxy nanocomposite coatings using inorganic nanoparticles for enhanced thermo-mechanical properties: a comparative study." *Journal of Coatings and Technology Research* 13, (September 2015): 159-169. doi:10.1007/s11998-015-9736-6.

- [15] Stambolova I, Yordanov S, Lakov L, Vassilev S, Blaskov V and Jivov B. "Preparation of sol-gel SiO₂ coatings on steel and their corrosion resistance." Proceedings of the 13th National Congress on Theoretical and Applied Mechanics, Sofia, Bulgaria. (September 2017).
- [16] Awizar, Denni Asra, Norinsan Kamil Othman, Azman Jalar, Abdul Razak Daud, I. Abdul Rahman, and N. H. Al-Hardan. "Nanosilicate extraction from rice husk ash as green corrosion inhibitor." *International Journal of Electrochemical Science* 8, no. 2 (2013): 1759-1769.
- [17] Attar, M.M., Matin, E. and Ramezanzadeh, B. "Investigation of modified nano-silica particles on the steel substrate corrosion protection properties of an epoxy nanocomposite loaded with polysiloxane surface." *Progress in Organic Coatings* 78, (January 2015): 395- 403. doi:10.1016/j.porgcoat.2014.07.004.
- [18] Wang H, Zhang C, Jiang C, Zhu L, Cui J, Han L, Chen M, Geng S and Wang F. "Evaluation of Glass Coatings with Various Silica Content Corrosion in a 0.5 M HCl Water Solution." *Crystals* 11, (2021): 346. doi:10.3390/cryst11040346.
- [19] Kazemi, M., I. Danaee, and D. Zaarei. "Deposition and Corrosion Behavior of Silicate Conversion Coatings on Aluminum Alloy 2024." *Materialwissenschaft Und Werkstofftechnik* 45, no. 7 (July 2014): 574–581. doi:10.1002/mawe.201400212.
- [20] Cheng L, Lou F, and Guo W. "Corrosion protection of the potassium silicate conversion coating." *Vacuum* 176, (June 2020): 109325. doi:10.1016/j.vacuum.2020.109325.
- [21] Bahri H, Danaee I, Rashed G, Zaarei D. " Effect of silica ratio on the corrosion behavior of nano-silica potassium silicate coatings on aluminum alloy 2024" *Journal of Materials Engineering and Performance* 2, (2015): 839-847. doi:10.1007/s11665-014-1325-9.
- [22] Dela Cruz, V.G., Tapia, A.K.G., Peralta, M.M., Almeda, R.A., Peralta, E.K., Sundo, M.B., Zafra, R.G. and Madlangbayan, M.S. "Investigation on performance of epoxy coated steels with nano-SiO₂ and polyaniline composite using complex impedance spectroscopy." *International Journal of Geomate* 64, (December 2019): 49-54. doi:10.21660/2019.64.42047.
- [23] Ruzgal, J.J.C., Suministrado, D.C., Amongo, R.M.C., Peralta, E.K., Quicoy, C.B. and Peralta, M.M. "Soil-to-Metal Friction, Soil Adhesion and Characterization of Nanosilica-Enhanced Coating Material for Cold-Rolled Steel." *Philippine Journal of Agricultural and Biosystems Engineering* 16, (January 2020): 3-16. doi:10.48196/016.01.2020.01.
- [24] ASTM G1 -2017 Standard Practice for Preparing, Cleaning, and Evaluating Corrosion Test Specimens. ASTM International, 100 Barr Harbor Drive, PO Box C700, West Conshohocken, PA 19428-2959, United States.
- [25] Grossi, M. and Ricco, B. "Electrical impedance spectroscopy (EIS) for biological analysis and food characterization: a review." *Journal of Sensors and Sensor Systems* 6, (2017): 303-325. doi:10.5194/jsss-6-303-2017.